Engineering mobility in quasiperiodic lattices with exact mobility edges

Zhenbo Wang [1], Yu Zhang,[2,3] Li Wang [1,*] and Shu Chen [2,3,†]

[1]*Institute of Theoretical Physics, State Key Laboratory of Quantum Optics and Quantum Optics Devices,*
Collaborative Innovation Center of Extreme Optics, Shanxi University, Taiyuan 030006, People's Republic of China
[2]*Beijing National Laboratory for Condensed Matter Physics, Institute of Physics, Chinese Academy of Sciences, Beijing 100190, China*
[3]*School of Physical Sciences, University of Chinese Academy of Sciences, Beijing 100049, China*

We investigate the effect of an additional modulation parameter δ on the mobility properties of quasiperiodic lattices described by a generalized Ganeshan-Pixley-Das Sarma model with two onsite modulation parameters. For the case with bounded quasiperiodic potential, we unveil the existence of self-duality relation, independent of δ. By applying Avila's global theory, we analytically derive Lyapunov exponents in the whole parameter space, which enables us to determine mobility edges or anomalous mobility edges exactly. Our analytical results indicate that the mobility edge equation is described by two curves and their intersection with the spectrum gives the true mobility edge. Tuning the strength parameter δ can change the spectrum of the quasiperiodic lattice, and thus engineers the mobility of quasiperiodic systems, giving rise to completely extended, partially localized, and completely localized regions. For the case with unbounded quasiperiodic potential, we also obtain the analytical expression of the anomalous mobility edge, which separates localized states from critical states. By increasing the strength parameter δ, we find that the critical states can be destroyed gradually and finally vanish.

I. INTRODUCTION

In condensed matter physics, mobility is a fundamental property of physical systems, which refers to the ability of a particle, such as an electron, to move through a material. In metal, it is responsible for the transport properties such as conductivity and resistance. In the context of semiconductors, it is an important parameter that determines the performance of electronic devices. Generally, mobility is influenced by factors like crystal structures, interactions, defects, and impurities, among others. More than 60 years ago, Anderson in his seminal work [1] investigated the role that the disordered onsite potential played on the mobility of particles in certain random lattices. From then on, Anderson localization [1,2] has attracted large and broad attention worldwide. Typically, for three-dimensional systems subjected to disorder of finite strength, localized and extended eigenstates can coexist in the energy band. Two intervals in the energy dimension corresponding to eigenstates with different mobility property are separated by a critical energy value, namely, the mobility edge [3]. Tuning the strength of disorders may shift the value of mobility edge. Accordingly, the proportion between extended and localized eigenstates may also change, finally leading to the modulation of system's mobility.

While mobility edge is usually absent for the above-mentioned uncorrelated disorders in low-dimensional systems [2,4], one-dimensional (1D) quasiperiodic systems offer an appealing platform to study localization-delocalization transition [5–11] and mobility edge [12–15]. Among these, the most famous one is the Aubry-André (AA) model [5], which analytically demonstrates the existence of localization-delocalization transition by utilizing the self-duality property. Subsequently, various generalizations to the standard AA model confirmed the existence of mobility edge in 1D quasiperiodic lattices, for example, lattice models with slowly varying quasiperiodic potentials [16,17], generalized AA model [12], incommensurate lattices with exponentially decaying hoppings [18], and the recently proposed mosaic model [14]. Hidden duality is revealed and simple ansatz is proposed to estimate the mobility edge for a variety of generic quasiperiodic models [19–23]. So far, the existence of mobility edges in low-dimensional systems has been demonstrated in various models [13,14,24–40]. Notably, potential applications of mobility edges in quantum devising like quantum thermal machine [41] and current rectifications [42,43] have been explored. Very recently, the concept of mobility edge has found its new territory in the emerging field of non-Hermitian physics [44–52].

In this work, we study quasiperidoic lattices described by a generalized Ganeshan-Pixley-Das Sarma (GPD) model with two tunable strength parameters of quasiperiodical potential. In comparison with the GPD model proposed by Ganeshan *et al.* [12], also referred as generalized AA model model in references, our model includes an additional modulation parameter δ [see Eq. (2)]. By applying Avila's global theory, we analytically derive the Lyapunov exponent in the whole parameter space, which enables us to determine the mobility edge exactly. Our analytical results indicate that the mobility edge equation is independent of δ and generally described by two curves, whose intersection with the spectrum of system

gives the true mobility edges. Tuning the strength parameter δ can change the spectrum of the quasiperiodic lattice, and thus provides a scheme to engineer the mobility of quasiperiodic systems. In this manner, with the anchored mobility edge as a separation, the ratio of eigenstates on both sides then is changed, leading to the engineering of system's mobility. Numerically calculating inverse participation ratios (IPRs) and Lyapunov exponents, we demonstrate that eigenstates of the system with bounded quasiperiodic potential successively cross the stationary mobility edge and undergo three scenarios, namely, completely extended, partially localized, and completely localized. For the case with unbounded quasiperiodic potential, we also obtain the analytical expression of the anomalous mobility edge, which separates localized states from critical states. By increasing the strength of δ, we find that the critical states are destroyed gradually and finally vanish.

The paper is organized as follows. First, we introduce our model in Sec. II A. Subsequently, in Sec. II B, we unveil the existence of self-duality relation for the system with bounded quasiperiodic potentials, independent of the modulation parameter δ. In Sec. II C, by applying Avila's global theory, we derive analytically the expression of Lyapunov exponent and mobility edge. In Sec. II D, we discuss the engineering of mobility and further verify our analytical results by numerically calculating the inverse participation ratios and Lyapunov exponents. The unbounded potential case is discussed in Sec. II E. Discussion on experimental design of the model is mentioned in Sec. II F. Finally, we give a summary in Sec. III.

II. MODEL AND RESULTS

A. Model

We consider a one-dimensional quasiperiodic lattice described by the following eigenvalue equation:

$$t(\phi_{n-1} + \phi_{n+1}) + V_n(\lambda, \delta, \alpha)\phi_n = E\phi_n, \quad (1)$$

with

$$V_n(\lambda, \delta, \alpha) = \frac{\lambda \, \cos(2\pi nb + \theta) + \delta}{1 - \alpha \, \cos(2\pi nb + \theta)}, \quad (2)$$

where n is the index of lattice site, and t is the nearest-neighbor hopping amplitude. The quasiperiodic potential is regulated by two modulation parameters λ, δ and a deformation parameter α. The parameter θ denotes a phase factor and b is an irrational number responsible for the quasiperiodicity of the onsite potential. To be concrete, in this work we choose $b = (\sqrt{5} - 1)/2$, however, the obtained results are also valid for any other choice of the irrational number b. For convenience, we shall set $t = 1$ as the energy unit in the following calculation.

When $\delta = 0$, the model reduces to the generalized AA model (GPD model) studied in Ref. [12], for which an exact mobility $\alpha E = 2 \, \text{sgn}(\lambda)|t| - \lambda$ is identified by the existence of a generalized duality symmetry for the case of $\alpha \in (-1, 1)$. On the other hand, the limit of $\lambda = 0$ was recently studied in Ref. [36] for the unbounded case $\alpha > 1$. The onset of anomalous mobility edges at the energies $E = \pm 2|t|$ is unveiled via the calculation of the Lyapunov exponent.

In this work, we shall consider the general case in the presence of both λ and δ terms. For the bounded case with $\alpha \in (-1, 1)$, we unveil the existence of a self-dual symmetry even in the presence of δ term, which enables us to get an expression of mobility edge. By applying Avila's global theory, we can derive the mobility edges and anomalous mobility edges analytically by calculating the Lyapunov exponents for both cases of $|\alpha| < 1$ and $|\alpha| > 1$.

B. Self-duality relation

At first, we consider the case of $\alpha \in (-1, 1)$ and demonstrate the existence of a generalized duality symmetry for the model with the quasiperiodic potential (2) under a generalized dual transformation, from which we can derive the exact mobility edges by searching the self-duality relation. Following Ref. [12], we define

$$\chi_n(\beta, \theta) \equiv \frac{\sinh \beta}{\cosh \beta - \cos(2\pi nb + \theta)}.$$

Since Eq. (2) can be represented as

$$V_n(\lambda, \delta, \alpha) = -\frac{\lambda}{\alpha} + \frac{\frac{\lambda}{\alpha} + \delta}{1 - \alpha \, \cos(2\pi nb + \theta)}, \quad (3)$$

the model described by Eqs. (1) and (2) can be straightforwardly rewritten into a form as

$$t(\phi_{n-1} + \phi_{n+1}) + G\chi_n(\beta, \theta)\phi_n = (E + \lambda \cosh \beta)\phi_n, \quad (4)$$

in which β is defined as $\cosh \beta \equiv 1/\alpha$ for $\alpha \in (0, 1)$, and the parameter G is given by $G = (\lambda \cosh \beta + \delta) \coth \beta$.

By using a well-established mathematical relation [12] as follows:

$$\frac{\sinh \beta}{\cosh \beta - \cos(2\pi nb + \theta)} = \sum_{r=-\infty}^{\infty} e^{-\beta|r|} e^{ir(2\pi nb + \theta)}, \quad (5)$$

we can implement consecutively three transformations to recover Eq. (4) into its initial form. Define $u_p = \sum_n e^{in(2\pi bp + q\pi)}\phi_n$, where $\sum_n$ is short for $\sum_{n=-\infty}^{\infty}$ and q is an integer. Multiplying $e^{in(2\pi bp + q\pi)}$ with both sides of Eq. (4) and performing a summation, we get

$$\omega \chi_p^{-1}(\beta_0, 0)e^{p\theta}u_p = G \sum_r e^{-\beta|p-r|} e^{r\theta}u_r, \quad (6)$$

where β_0 is defined through relation $E + \lambda \cosh \beta \equiv (-1)^q 2t \cosh \beta_0$ and ω is defined as $\omega \equiv (-1)^q 2t \sinh \beta_0$. Subsequently, we move on to implement the second transformation $v_m = \sum_p e^{ip(2\pi bm + \theta + q\pi)} \chi_p^{-1}(\beta_0, 0)u_p$. By multiplying $e^{ip(2\pi bm + \theta + q\pi)}$ with both sides and making a sum over p, Eq. (6) is correspondingly transformed into

$$\omega \chi_m^{-1}(\beta, q\pi)v_m = G \sum_r e^{-\beta_0|m-r|}v_r. \quad (7)$$

Then it comes to the last step where the transformation is defined as $z_k = \sum_m e^{im(2\pi bk + \theta)}v_m$. We multiply Eq. (7) by $e^{im(2\pi bk + \theta)}$ and sum over m. Finally, one obtains the following tight-binding model about z_k:

$$t(z_{k+1} + z_{k-1}) + G\frac{\sinh \beta}{\sinh \beta_0}\chi_k(\beta_0, \theta)\, z_k = (-1)^q 2t \, \cosh \beta \, z_k. \quad (8)$$

It is not difficult to notice that Eq. (8) can be managed to be equivalent to Eq. (4), if one lets $\beta = \beta_0$. Accordingly, we have $E + \lambda \cosh \beta = (-1)^q 2t \cosh \beta$, which in terms of the original parameter α is

$$\alpha E = (-1)^q 2t - \lambda. \qquad (9)$$

Since q may take even or odd integers, this actually gives out the analytical formula of a pair of exact mobility edges. As for the other case $\alpha \in (-1, 0)$, one can also arrive at Eq. (9) by conducting similar derivations as above.

C. Analytical formula of the exact mobility edge

Next we apply Avila's global theory [53] to calculate the Lyapunov exponent and derive the exact mobility edge [54,55]. For convenience, we will absorb t into λ and E in the derivation process by setting $t = 1$.

For the spectral problem with incommensurate potential, the Lyapunov exponent $\gamma(E)$ is defined as

$$\gamma(E) = \lim_{L \to \infty} \frac{1}{L} \ln ||T_L(\theta)||,$$

where $||T_L(\theta)||$ is the norm of the 2×2 transfer matrix $T_L(\theta)$, given by

$$T_L(\theta) = \prod_{n=1}^{L} M_n, \qquad (10)$$

in which

$$M_n = \begin{pmatrix} E - V_n & -1 \\ 1 & 0 \end{pmatrix}, \qquad (11)$$

with V_n given by Eq. (2).

We adopt the conventional procedure to calculate Lyapunov exponent. First, we need to complex the phase, i.e., letting $\theta \to \theta + i\epsilon$. In order to apply global theory more conveniently, we introduce a new matrix $\widetilde{M}_j$, which can be written as

$$\widetilde{M}_j(\theta) = [1 - \alpha \cos(2\pi j b + \theta)] M_j. \qquad (12)$$

Then the transfer matrix for $\widetilde{M}_j(\theta)$ can be expressed as

$$\widetilde{T}_L(E, \theta) = \prod_{j=1}^{L} \widetilde{M}_j(\theta).$$

And the Lyapunov exponent about $\widetilde{T}_L(E, \theta + i\epsilon)$ is

$$\tilde{\gamma}(E, \theta + i\epsilon) = \lim_{L \to \infty} \frac{1}{L} \ln ||\widetilde{T}_L(E, \theta + i\epsilon)||.$$

In the limit of $L \to \infty$, we can replace the sum of j by an integral

$$\tilde{\gamma}(E, \theta + i\epsilon) = \frac{1}{2\pi} \int \ln ||\widetilde{T}_L(E, \theta + i\epsilon)|| d\theta.$$

Then it follows

$$\gamma(E, \epsilon) = \tilde{\gamma}(E, \epsilon) - \frac{1}{2\pi} \int \ln[1 - \alpha \cos(\theta + i\epsilon)] d\theta. \qquad (13)$$

In this part, we focus on the case $-1 < \alpha < 1$ and the result of the integral in Eq. (13) is

$$\frac{1}{2\pi} \int \ln[1 - \alpha \cos(\theta + i\epsilon)] d\theta = \ln \frac{1 + \sqrt{1 - \alpha^2}}{2},$$

if $|\epsilon| < \ln |\frac{1 + \sqrt{1 - \alpha^2}}{\alpha}|$. From Eq. (13), we can find that $\gamma(E, \epsilon)$ and $\tilde{\gamma}(E, \epsilon)$ has the same slope about ϵ when $|\epsilon| < \ln |\frac{1 + \sqrt{1 - \alpha^2}}{\alpha}|$.

In the large-ϵ limit, we get

$$\widetilde{T}_L(E, \epsilon) = \prod_{j=1}^{L} \frac{1}{2} e^{-i2\pi b j} e^{|\epsilon|} \begin{pmatrix} -\alpha E - \lambda & \alpha \\ -\alpha & 0 \end{pmatrix} + o(1). \qquad (14)$$

According to the Avila's global theory, $\tilde{\gamma}(E, \epsilon)$ is a convex, piecewise linear function about $\epsilon \in (-\infty, \infty)$. Combined with the result of Eq. (14), we can see that the slope about ϵ is always 1. Thus, the Lyapunov exponent about $\widetilde{T}_L(E, \theta + i\epsilon)$ can be written as

$$\tilde{\gamma}(E, \epsilon) = |\epsilon| + \ln f(E)$$

for large enough ϵ, where

$$f(E) = \left| \frac{|\alpha E + \lambda| + \sqrt{(\alpha E + \lambda)^2 - 4\alpha^2}}{4} \right|.$$

Considering the convexity of the Lyapunov exponent, the slope of $\gamma(E, \epsilon)$ might be 1 or 0 in the region $0 \leqslant |\epsilon| < \ln |\frac{1 + \sqrt{1 - \alpha^2}}{\alpha}|$. Besides, the slope of $\gamma(E, \epsilon)$ in a neighborhood of $\epsilon = 0$ is nonzero if the energy E is in the spectrum.

Therefore, when E is in the spectrum,

$$\tilde{\gamma}(E, \epsilon) = |\epsilon| + \ln f(E), \qquad (15)$$

for any $\epsilon \in (-\infty, \infty)$. Based on Eq. (13) and the non-negativity of Lyapunov exponent $\gamma(E, \epsilon)$, we have

$$\gamma(E, 0) = \max \left\{ \ln \frac{2f(E)}{1 + \sqrt{1 - \alpha^2}}, 0 \right\}. \qquad (16)$$

Then the mobility edge can be determined by $\gamma(E) = 0$, which gives rise to

$$\left| \alpha \frac{E}{t} + \frac{\lambda}{t} \right| = 2, \qquad (17)$$

where we have already explicitly included t.

Although Eq. (17) takes a different form from Eq. (9), it can be checked that they are actually equivalent. This result suggests that the mobility edges may be composed of two curves. The appearance of the mobility edge depends on another condition: a true mobility edge exists only if these curves are within the energy spectrum. Therefore, the energy spectrum and the mobility edge equation together determine the mobility properties of the system. In order to determine which curve determines the mobility edge for different parameters, we import the operator theory and give more accurate results. By comparing the expression of curves with the range of the physical possible energy spectrum (more details can be found in Appendix A), we arrive at the expression

$$E_c = \frac{2 \operatorname{sgn}(\lambda + \delta\alpha)|t| - \lambda}{\alpha}. \qquad (18)$$
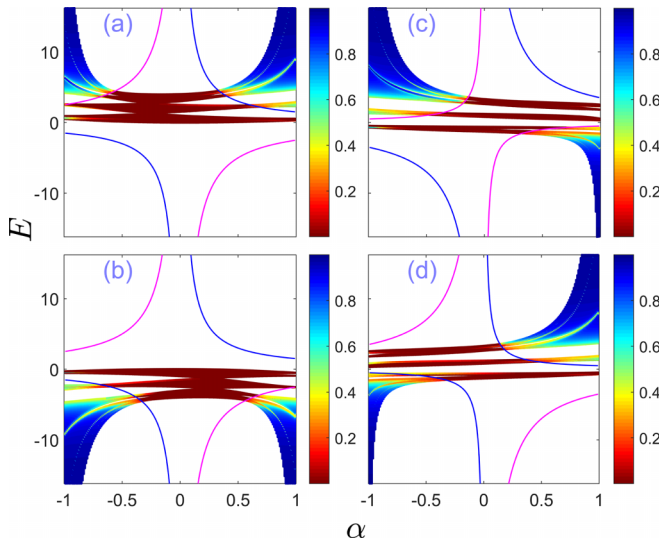
FIG. 1. Numerical spectrum E of the model in Eq. (1) as a function of α with model parameters $L = 10\,000$, $\theta = 0$, and $t = 1$. The IPR of each eigenstate is also calculated, which is indicated by the color of each eigenvalue in the spectrum. The lines in magenta and blue are exact mobility edges predicted by analytical formula (9). (a) $\lambda = 0.5$, $\delta = 2$, (b) $\lambda = 0.5$, $\delta = -2$, (c) $\lambda = -1.5$, $\delta = 1$, (d) $\lambda = 1.5$, $\delta = 1$.

When $\delta = 0$, we see that the mobility edge reduces to $E_c = \frac{2\,\mathrm{sgn}(\lambda)|t| - \lambda}{\alpha}$, consistent with the result in Ref. [12]. In this case, for a given λ parameter, e.g., $\lambda > 0$ and $t = 1$, the mobility edge is only determined by the curve $E_c = \frac{2-\lambda}{\alpha}$. However, in the presence of nonzero δ, the mobility edge can be given by either $E_c = \frac{2-\lambda}{\alpha}$ or $E_c = \frac{-2-\lambda}{\alpha}$ depending on the value of $\lambda + \delta\alpha$, as displayed in Fig. 1.

To gain an intuitive understanding, we display some numerical results in Fig. 1 for system with various parameters λ and δ, in which we display the energy spectrum versus α and plot the mobility edges given by Eq. (9) and the inverse participation ratios (IPRs) [56] as a function of α. The IPR for an eigenstate with eigenvalue E is given as

$$\mathrm{IPR}(E_i) = \frac{\sum_n |\phi_n(E_i)|^4}{\left(\sum_n |\phi_n(E_i)|^2\right)^2}, \qquad (19)$$

where E_i is the ith energy eigenvalue. For an extended eigenstate, the probability tends to be distributed evenly among the lattice, thus, the IPR is expected to be the order of $1/L$. While for a localized eigenstate, the probability is usually well confined to a few lattice sites, therefore the IPR approaches 1 in the limiting case. It is shown that the localized and extended regions are separated by the mobility edge. In Figs. 1(a) and 1(b), the mobility edges are determined by different curves because the sign of $\lambda + \delta\alpha$ is changed in the process of adjusting α from -1 to 1. In contrast, the mobility edges in Figs. 1(c) and 1(d) are determined by only one curve because adjusting α does not change the sign of $\lambda + \delta\alpha$.

D. Engineering the mobility property

Although the equation of mobility edges are simply two straight lines described by $E = \frac{2}{\alpha} - \frac{\lambda}{\alpha}$ and $E = -\frac{2}{\alpha} - \frac{\lambda}{\alpha}$,
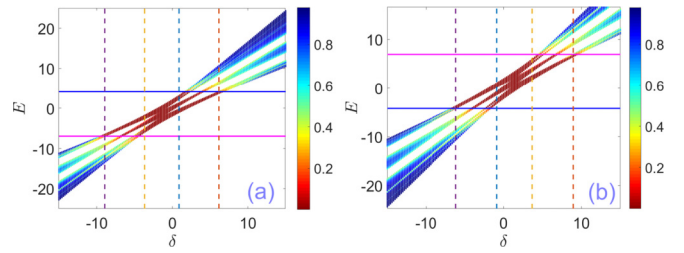
FIG. 2. Numerical spectrum E of the model in Eq. (1) as a function of δ with different parameters. (a) $\lambda = -0.5$, $\alpha = -0.36$. (b) $\lambda = -0.5$, $\alpha = 0.36$. We choose $L = 10\,000$, $\theta = 0$, and $t = 1$ in all cases. The lines in magenta and blue are exact mobility edges predicted by analytical formula (9). The dashed lines denote transition points separating different regions.

which are independent of δ, tuning δ can change the spectrum of the system dramatically. By tuning δ, we can access five different regions as shown in Fig. 2.

By comparing the energy spectrum and the equation of mobility edges, we can approximately obtain transition points separating these different regions of δ (details about the transition points can be found in Appendix B). For the case of $-1 < \alpha < 0$, as shown in Fig. 2(a), the five different regions are as follows: (i) For $-\infty < \delta < -\frac{\lambda}{\alpha} + \frac{2(1-\alpha)}{\alpha}$, all the eigenstates are localized. (ii) For $-\frac{\lambda}{\alpha} + \frac{2(1-\alpha)}{\alpha} < \delta < -\frac{\lambda}{\alpha} + \frac{2(1+\alpha)^2}{\alpha}$, there is a mobility edge determined by $E = -\frac{\lambda}{\alpha} + \frac{2}{\alpha}$, below which the states are localized, whereas above which the states are extended. (iii) For $-\frac{\lambda}{\alpha} + \frac{2(1+\alpha)^2}{\alpha} < \delta < -\frac{\lambda}{\alpha} - \frac{2(1+\alpha)^2}{\alpha}$, all the eigenstates are extended. (iv) For $-\frac{\lambda}{\alpha} - \frac{2(1+\alpha)^2}{\alpha} < \delta < -\frac{\lambda}{\alpha} - \frac{2(1-\alpha)}{\alpha}$, there is a mobility edge determined by $E = -\frac{\lambda}{\alpha} - \frac{2}{\alpha}$, below which the states are extended, whereas above which the states are localized. (v) For $-\frac{\lambda}{\alpha} - \frac{2(1-\alpha)}{\alpha} < \delta < +\infty$, all the eigenstates are localized. For the case of $0 < \alpha < 1$, as shown in Fig. 2(b), the five different regions are as follows: (i) For $-\infty < \delta < -\frac{\lambda}{\alpha} - \frac{2(1+\alpha)}{\alpha}$, all the eigenstates are localized. (ii) For $-\frac{\lambda}{\alpha} - \frac{2(1+\alpha)}{\alpha} < \delta < -\frac{\lambda}{\alpha} - \frac{2(1-\alpha)^2}{\alpha}$, there is a mobility edge determined by $E = -\frac{\lambda}{\alpha} - \frac{2}{\alpha}$, below which the states are localized, whereas above which the states are extended. (iii) For $-\frac{\lambda}{\alpha} - \frac{2(1-\alpha)^2}{\alpha} < \delta < -\frac{\lambda}{\alpha} + \frac{2(1-\alpha)^2}{\alpha}$, all the eigenstates are extended. (iv) For $-\frac{\lambda}{\alpha} + \frac{2(1-\alpha)^2}{\alpha} < \delta < -\frac{\lambda}{\alpha} + \frac{2(1+\alpha)}{\alpha}$, there is a mobility edge determined by $E = -\frac{\lambda}{\alpha} + \frac{2}{\alpha}$, below which states are extended, whereas above which states are localized. (v) For $-\frac{\lambda}{\alpha} + \frac{2(1+\alpha)}{\alpha} < \delta < +\infty$, all the eigenstates are localized.

To see how the mobility is engineered by the strength of δ, we show the change of IPRs and Lyapunov exponents of all eigenstates in Fig. 3 by choosing several typical parameters corresponding to Fig. 2(a). The Lyapunov exponents [17] (LEs) for finite-size lattices can be numerically calculated by using [57,58]

$$\gamma(E_i) = \frac{1}{L-1} \sum_{j \neq i} \ln \left| \frac{E_i - E_j}{t} \right|. \qquad (20)$$
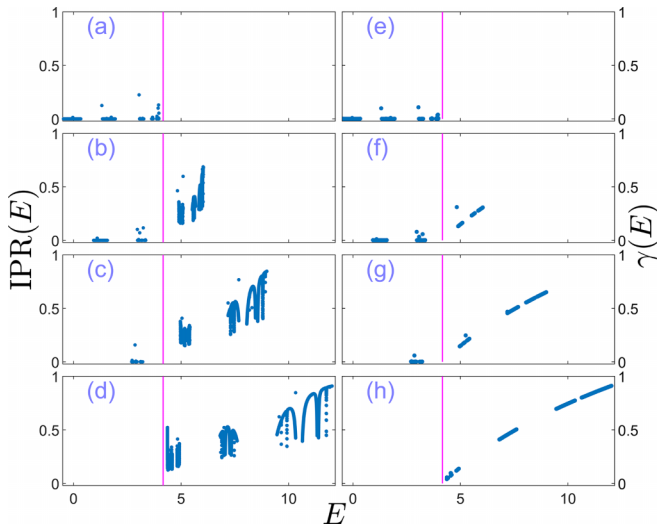
FIG. 3. Engineering the system's mobility by varying the strength parameter δ while mobility edge is kept fixed by the strength parameter λ. The left column shows the inverse participation ratios (IPRs) of all single-particle eigenstates for different values of δ. The lattice size is $L = 10\,000$ with parameters $t = 1$, $\theta = 0$, $\alpha = -0.36$, and $\lambda = -0.5$. The right column gives the corresponding Lyapunov exponents (LEs). (a), (e) $\delta = 1.5$, (b), (f) $\delta = 3.0$, (c), (g) $\delta = 5.0$, (d), (h) $\delta = 7.0$. The vertical line in [(a)–(h)] denotes position of the anchored mobility edge.

It is well known that Lyapunov exponent is the inverse of localization length, thus, for an extended eigenstate it approaches to a vanishing value as the lattice size L increases. On the other hand, the Lyapunov exponent is nonzero for localized states. The IPRs for all single-particle eigenstates under different strengths of δ are shown in Figs. 3(a)–(d) and the LEs are correspondingly given in Figs. 3(e)–(h). For all of them the strength of λ is fixed at $\lambda = -0.5$. The lattice size is $L = 10\,000$ and other parameters are $\alpha = -0.36$ and $\theta = 0$. From top to bottom, the corresponding strengths of the second quasiperiodic potential are $\delta = 1.5$, 3.0, 5.0, and 7.0. It is clearly shown that as the strength of δ is modulated from $\delta = 1.5$ to 7.0, the system is engineered to undergo different situations, initially wholly extended, then partially localized, and at last completely localized. Notably, during the whole process, the mobility edge denoted by vertical line in Fig. 3 is fixed and rather robust against the variation of the strength of δ. As the strength of δ is varied, single-particle eigenstates change their mobility properties by leapfrogging the fixed mobility edge consecutively, one by one.

In the above calculation, δ is chosen as an independent parameter. Nevertheless, we can also choose δ as a function of λ. Although the form of $\delta(\lambda)$ does not change the mobility edge equation, it can modulate the structure of spectrum and thus enable us engineering the mobility properties of the quasiperiodic lattices. In Figs. 4(a) and 4(b), we display the energy spectrum and corresponding IPRs versus λ for systems with $\delta = \frac{1}{\alpha} \sin(\lambda)$ and $\delta = \frac{\lambda}{\alpha} \sin(\lambda)$, respectively. While the extended states and the mobility edges occur only in a region around $\lambda = 0$ as shown in Fig. 4(a), we find that the mobility edges occur periodically in Fig. 4(b) with the increase of λ. Intuitively, periodically occurring mobility
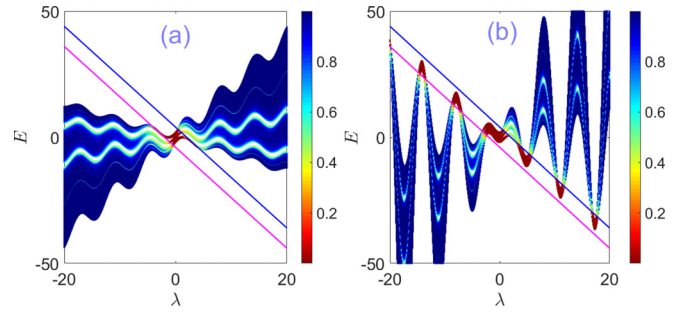
FIG. 4. Examples of energy spectrum engineering with the freedom granted by the modulation of δ as a function of λ. IPR is indicated by the color of the eigenvalue point. The lattice size is $L = 10\,000$. (a) $\delta = \frac{1}{\alpha} \sin(\lambda)$, (b) $\delta = \frac{\lambda}{\alpha} \sin(\lambda)$. Other parameters are $\alpha = 0.5$, $t = 1$, $\theta = 0$.

edges can be attributed to the periodical occurrence of zero points of $\frac{\lambda}{\alpha} + \delta(\lambda)$. According to the expression of Eq. (3), when $\frac{\lambda}{\alpha} + \delta(\lambda) = 0$, the quasiperiodic potential vanishes, and the corresponding eigenstates must be extended states. When $\frac{\lambda}{\alpha} + \delta(\lambda) \neq 0$, localized states may occur if the energy spectrum exceeds the mobility edge curves.

E. Anomalous mobility edges for the case of $|\alpha| > 1$

For the case of $|\alpha| > 1$, the quasiperiodic potential given by Eq. (2) is in principle an unbounded potential, which, however, does not diverge at any lattice site for a finite-size lattice. According to the Simon-Spencer theorem [59], extended states are forbidden for an unbounded quasiperiodic potential, and thus the self-duality mapping does not work. Nevertheless, we can use Avila's global theory for unbounded quasiperiodic operators to derive the analytical expression of anomalous mobility edges [36,39]. The derivation of mobility edges for $|\alpha| > 1$ is similar to the case of $|\alpha| < 1$ until Eq. (13). The result of the integral in Eq. (13) for $|\alpha| > 1$ is

$$\frac{1}{2\pi} \int \ln[1 - \alpha \cos(\theta + i\epsilon)]d\theta = |\epsilon| + \ln\left(\frac{\alpha}{2}\right).$$

Thus, we can get the Lyapunov exponent in the large-ϵ limit as

$$\gamma(E, \epsilon) = \ln\left(\frac{2f(E)}{\alpha}\right)$$

for any ϵ. The Lyapunov exponent $\gamma(E, \epsilon)$ is independent of ϵ. Similar to the discussion in Ref. [36], there is an anomalous mobility edge determined by $\gamma(E) = 0$. Here the anomalous mobility edge means an edge separating localized states and critical states. Through straightforward calculations, we arrive at an exact analytical formula of the anomalous mobility edge as

$$E_c = \pm 2|t| - \frac{\lambda}{\alpha}. \tag{21}$$

Before proceeding with further discussion, we set $t = 1$ for convenience. In regions of $E > 2 - \frac{\lambda}{\alpha}$ and $E < -2 - \frac{\lambda}{\alpha}$, $\gamma(E) > 0$ and the eigenstates are localized eigenstates with localization length $\xi = 1/\gamma(E)$. In the region $-2 - \frac{\lambda}{\alpha} < E <$
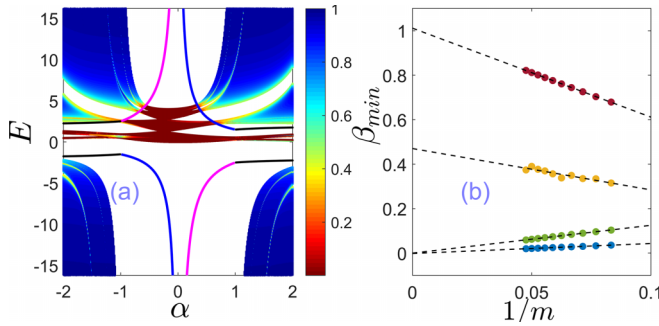
FIG. 5. (a) Mobility edges and anomalous mobility edges. The lattice size is $L = 10\,000$. Other parameters are $t = 1$, $\theta = 0$, $\delta = 2$, and $\lambda = 0.5$. The lines in magenta and blue are exact mobility edges predicted by analytical formula (9). The lines in black are anomalous mobility edges predicted by analytical formula (21). (b) $\beta_{\min}$ as a function of the inverse Fibonacci index $1/m$ for different α. From top to bottom, data points in different colors represent extended eigenstates (in the energy interval $[\frac{2}{-\alpha} - \frac{\lambda}{\alpha}, \frac{2}{\alpha} - \frac{\lambda}{\alpha}]$) with $\alpha = 0.7$, critical eigenstates (in the energy interval $[-2 - \frac{\lambda}{\alpha}, 2 - \frac{\lambda}{\alpha}]$) with $\alpha = 1.5$, localized eigenstates (outside the energy interval $[\frac{2}{-\alpha} - \frac{\lambda}{\alpha}, \frac{2}{\alpha} - \frac{\lambda}{\alpha}]$) with $\alpha = 0.7$, localized eigenstates (outside the energy interval $[-2 - \frac{\lambda}{\alpha}, 2 - \frac{\lambda}{\alpha}]$) with $\alpha = 1.5$.

FIG. 6. Modulations of eigenstate properties by varying the strength parameter δ while the anomalous mobility edge is kept fixed by the strength parameter λ. The left column shows the inverse participation ratios (IPRs) of all single-particle eigenstates for different values of δ. The lattice size is $L = 10\,000$ with parameters $t = 1$, $\theta = 0$, $\alpha = -2$, and $\lambda = -0.5$. The right column gives the corresponding Lyapunov exponents (LEs). (a), (d) $\delta = 0$, (b), (e) $\delta = 2.0$, (c), (f) $\delta = 5.7$. The vertical lines in [(a)–(f)] denote positions of the anchored anomalous mobility edges given by Eq. (21).

$2 - \frac{\lambda}{\alpha}$, the energy spectrum is singular continuous and the eigenstates are critical.

Next we carry out numerical analysis to unveil the existence of anomalous mobility edges in the regime of $|\alpha| > 1$. In Fig. 5(a), we display the energy spectrum and corresponding IPRs versus α for both the regions of $|\alpha| < 1$ and $|\alpha| > 1$. In order to distinguish the extended eigenstates and critical eigenstates displayed in Fig. 5(a), we make multifractal analysis and calculate the scaling exponent $\beta_{\min}$. The multifractal analysis demands considering a series of finite systems with different sizes. We thus choose the system size L as the mth Fibonacci number F_m. The scaling exponent $\beta_{\min}$ can be extracted as follows. For a given wave function ψ_n^j, one can extract a scaling exponent β_n^j from the nth onsite probability $P_n^j = |\psi_n^j|^2 \sim (1/F_m)^{\beta_n^j}$. Here we use the minimum value $\beta_{\min}^j = \min_n(\beta_n^j)$ to characterize eigenstate properties. As the system size increases, $\beta_{\min}^j \rightarrow 1$ for the extended eigenstates, whereas $\beta_{\min}^j \rightarrow 0$ for the localized eigenstates. For the critical eigenstates, the $\beta_{\min}^j$ approaches to a value in the interval $(0,1)$. In order to reduce the fluctuations among different critical eigenstates, we define an average scaling exponent $\beta_{\min} = \frac{1}{L'} \sum_{j=1}^{L'} \beta_{\min}^j$, where L' is the number of eigenstates in the corresponding region. In Fig. 5(b), the numerical result of scaling analysis is shown. For the regime of $|\alpha| > 1$, there appear anomalous mobility edges. On the other hand, there are normal mobility edges for the regime of $|\alpha| < 1$.

From Eq. (21), we see that the pair of anomalous mobility edges is completely independent of δ. Thus, in the unbounded case, one is also granted a degree of freedom to engineer the system's spectrum while the position of the anomalous mobility edge is kept fixed. As the strength of δ varies,

certain eigenstates may hop across the anomalous mobility edge and the property of the eigenstate changes. In Fig. 6, we show this manner of modulations of eigenstate properties by numerically calculating IPRs (left column) and LEs (right coloumn) for all eigenstates. The two vertical lines denote the anomalous mobility edges predicted by Eq. (21). Data points in-between stand for critical eigenstates while those points outside denote localized eigenstates. From top to bottom, the strengths of the second quasiperiodic potential are $\delta = 0$, 2, and 5.7. It is clearly shown that as δ varies, the critical states are killed gradually and finally all critical states vanish. For the unbounded case of $|\alpha| > 1$, we notice that the spectrum is very wide and thus a region with all eigenstates being critical states is hard to be accessed by tuning δ, which is in contrast with the bounded case where a completely extended region is accessible.

F. Experimental prospects

The model considered in this work may be experimentally implemented with the state-of-the-art techniques. Thanks to the rapid advancement in experimental techniques, a lot of quasiperiodic potentials in reduced dimensions have already been successfully realized in experiments based on ultracold atoms [10,11,13,60–63]. To realize the model in Eq. (1), one may hopefully work along the lines of synthetic lattices in momentum space [62,64]. In that scheme, a pair of counterpropagating lasers is used to drive Bragg transitions which can change the atomic momentum discretely with fixed increments. One of the lasers has a single frequency while the other has many different components. Together, the pair of lasers drive a set of two-photon Bragg transitions, and thus a synthetic lattice in momentum space is

created. What is particularly commendable of the scheme is the ability of generic site energy control [62]. By independently modulating the strength, phase, and detuning for each of the Bragg transitions, the site-to-site energy difference in the synthetic lattice is engineered. Taking advantage of this ability, the quasiperiodic potential in Eq. (2) is then within the reach of experiment experts. Alternatively, one can adopt the strategy of Ganeshan-Pixley-Das Sarma [12] to experimentally realize the model (1) in real space other than momentum space mentioned above. The onsite potential in Eq. (2) can be expressed as a sum of cosine Fourier series. Each cosine term is AA-model like and realizable in experiment. Thus, one can manage to obtain the quasiperiodic potential in Eq. (2) by superimposing several cosine terms together, especially when considering α with small values. Additionally, the photonic waveguide platform is also a good candidate to realize quasiperiodic models [11,65]. Moreover, it is particularly convenient to further implement Floquet engineering for this setup.

III. SUMMARY

In summary, we study 1D quasiperiodic lattices described by a generalized GPD model with an additional tunable parameter δ in the whole parameter space, including cases with both the bounded and unbounded quasiperiodic potentials. By applying Avila's global theory, we derive the analytical expression of Lyapunov exponent, which permits us to get the exact expression of mobility edges and anomalous mobility edges. Although the mobility edge equation and anomalous mobility edge equation do not include the introduced parameter δ explicitly, the parameter can modulate the energy spectrum and thus provides a way to engineering the mobility properties of the system. By numerically calculating the IPRs and Lyapunov exponents, we show that the mobility can be flexibly engineered by modulating the strength of a new parameter while the mobility edge equation is kept unchanged. For the bounded case, the modulation of δ can lead to completely extended, partially localized, and completely localized regions. For the unbounded case, the modulation of δ can only lead to partially localized and completely localized states, whereas a completely critical region is hard to be accessed. Our study unveils the richness of quasiperiodic localization and provides a scheme to engineer the mobility properties of quasiperiodic lattices.

APPENDIX A: ACCURATE EXPRESSION OF THE MODEL'S MOBILITY EDGE FOR THE CASE WITH |α| < 1

The mobility edge can be determined by letting Lyapunov exponent $\gamma(E) = 0$, which gives

$$\left|\frac{\alpha E + \lambda}{t}\right| = 2. \tag{A1}$$

To be specific, it consists of two parts,

$$E_{c1} = \frac{2|t| - \lambda}{\alpha}, \tag{A2}$$

$$E_{c2} = \frac{-2|t| - \lambda}{\alpha}. \tag{A3}$$

To get a more accurate formula for the mobility edge, one has to resort to operator theory. According to the operator theory, the range of the physical possible energy spectrum E of the model (1) can be estimated as $E \subseteq [-2|t| + \min(V_n), 2|t| + \max(V_n)]$.

Before proceeding, we note that the onsite potential can be rewritten as

$$V_n = \frac{\lambda/\alpha + \delta}{1 - \alpha \cos(2\pi nb + \theta)} - \lambda/\alpha. \tag{A4}$$

Thus, when $\lambda/\alpha + \delta > 0$ and $\alpha > 0$, we have

$$\{E\} \subseteq \left[-2|t| + \frac{\lambda/\alpha + \delta}{1 + \alpha} - \lambda/\alpha, 2|t| + \frac{\lambda/\alpha + \delta}{1 - \alpha} - \lambda/\alpha\right], \tag{A5}$$

while when $\lambda/\alpha + \delta > 0$ and $\alpha < 0$, we have

$$\{E\} \subseteq \left[-2|t| + \frac{\lambda/\alpha + \delta}{1 - \alpha} - \lambda/\alpha, 2|t| + \frac{\lambda/\alpha + \delta}{1 + \alpha} - \lambda/\alpha\right]. \tag{A6}$$

And when $\lambda/\alpha + \delta < 0$ and $\alpha > 0$, we have

$$\{E\} \subseteq \left[-2|t| + \frac{\lambda/\alpha + \delta}{1 - \alpha} - \lambda/\alpha, 2|t| + \frac{\lambda/\alpha + \delta}{1 + \alpha} - \lambda/\alpha\right], \tag{A7}$$

while $\lambda/\alpha + \delta < 0$ and $\alpha < 0$, we have

$$\{E\} \subseteq \left[-2|t| + \frac{\lambda/\alpha + \delta}{1 + \alpha} - \lambda/\alpha, 2|t| + \frac{\lambda/\alpha + \delta}{1 - \alpha} - \lambda/\alpha\right]. \tag{A8}$$

According to the above-obtained ranges of the energy spectrum E under four different cases, we can arrive at more accurate mobility edges by excluding the un-physical part.

First, we consider the case with $\lambda/\alpha + \delta > 0$ and $\alpha > 0$. In this case, it is obviously that $E_{c1} > E_{c2}$. And we have the following relation:

$$-2|t|\alpha + \frac{\lambda + \delta\alpha}{1 + \alpha} > -2|t|. \tag{A9}$$

So, accordingly, one can get

$$E_{c2} < -2|t| + \frac{\lambda/\alpha + \delta}{1 + \alpha} - \lambda/\alpha. \tag{A10}$$

This means that E_{c2} is even below the lower limit of the energy spectrum. So E_{c2} should be omitted and only E_{c1} is valid in this case.

Second, we turn to the case $\lambda/\alpha + \delta > 0$ and $\alpha < 0$, for which we have $E_{c2} > E_{c1}$. Noting that $\lambda + \delta\alpha < 0$, it is easy to find that the following relation is fulfilled:

$$2|t|(1 + \alpha)(1 - \alpha) > \lambda + \delta\alpha. \tag{A11}$$

Thus, we can see that E_{c1} is lower than the minimum of the model's energy spectrum E, i.e.,

$$E_{c1} < -2|t| + \frac{\lambda/\alpha + \delta}{1 - \alpha} - \lambda/\alpha. \tag{A12}$$

So in this case, E_{c1} is excluded and E_{c2} is kept.

Third, we consider the case $\lambda/\alpha + \delta < 0$ and $\alpha > 0$. In this case, we have $E_{c1} > E_{c2}$ and the relation

$$\frac{\lambda/\alpha + \delta}{1 + \alpha} < 0 < 2|t|\left(\frac{1}{\alpha} - 1\right). \tag{A13}$$

It is straightforward to arrive at

$$E_{c1} > 2|t| + \frac{\lambda/\alpha + \delta}{1 + \alpha} - \lambda/\alpha, \tag{A14}$$

which means E_{c1} is outside the range of the model's energy spectrum. Therefore, in this case, the model's mobility edge is determined by E_{c2}.

Fourth, we check the case $\lambda/\alpha + \delta < 0$ and $\alpha < 0$. Obviously, we have $E_{c2} > E_{c1}$ in this case. Also noting the relation

$$\frac{\lambda/\alpha + \delta}{1 - \alpha} < 0 < -2|t|\left(\frac{1}{\alpha} + 1\right), \tag{A15}$$

we can get

$$E_{c2} > 2|t| + \frac{\lambda/\alpha + \delta}{1 - \alpha} - \lambda/\alpha. \tag{A16}$$

This means E_{c2} is above the upper limit of the physical model's energy spectrum E. Therefore, the mobility edge in this case is determined by E_{c1}.

In summary, when $\alpha > 0$, the mobility edge can be described by

$$E_c = \frac{2\,\mathrm{sgn}(\lambda/\alpha + \delta)|t| - \lambda}{\alpha}, \tag{A17}$$

and on the other hand, for $\alpha < 0$, we have

$$E_c = \frac{-2\,\mathrm{sgn}(\lambda/\alpha + \delta)|t| - \lambda}{\alpha}. \tag{A18}$$

Furthermore, the mobility edge can be written in a briefer form

$$E_c = \frac{2\,\mathrm{sgn}(\alpha)\,\mathrm{sgn}(\lambda/\alpha + \delta)|t| - \lambda}{\alpha}. \tag{A19}$$

Finally, we arrive at

$$E_c = \frac{2\,\mathrm{sgn}(\lambda + \delta\alpha)|t| - \lambda}{\alpha}. \tag{A20}$$

APPENDIX B: TRANSITION POINTS BY TUNING δ

Here we focus on the interval $-1 < \alpha < 0$ and estimate the range of energy spectrum, while the discussion in the interval $0 < \alpha < 1$ is similar. For the discussion below, the hopping amplitude t is set to be 1. Observing the onsite potential (2), a special point is obvious: $\frac{\lambda}{\alpha} + \delta = 0$. At this point, the range of energy spectrum is $[-2, 2]$ and the eigenstates are always extended. For convenience, we define a new parameter $\Delta \equiv \frac{\lambda}{\alpha} + \delta$ from now on. In the following, we will discuss from two aspects.

(i) $\Delta > 0$. The energy spectrum only has cross points with the upper mobility edge line $E = -\frac{2}{\alpha} - \frac{\lambda}{\alpha}$. When Δ is small, the approximate range of energy spectrum spectrum is $[-2 + \frac{\Delta}{1-\alpha} - \frac{\lambda}{\alpha}, 2 + \frac{\Delta}{1+\alpha} - \frac{\lambda}{\alpha}]$. Thus, a transition point appears when the mobility edge line intersects with the energy spectrum. It is determined by

$$-\frac{2}{\alpha} = 2 + \frac{\Delta}{1 + \alpha}. \tag{B1}$$

So the transition point is given as

$$\Delta = -\frac{2(1 + \alpha)^2}{\alpha} \rightarrow \delta = -\frac{\lambda}{\alpha} - \frac{2(1 + \alpha)^2}{\alpha}. \tag{B2}$$

When Δ is large, all the eigenstates become localized states. In this regime, the range of energy spectrum is well approximated as $[\frac{\Delta}{1-\alpha} - \frac{\lambda}{\alpha}, \frac{\Delta}{1+\alpha} - \frac{\lambda}{\alpha}]$. And the transition point upon which all the states become localized is determined by

$$-\frac{2}{\alpha} = \frac{\Delta}{1 - \alpha} \tag{B3}$$

and the transition point is

$$\Delta = -\frac{2(1 - \alpha)}{\alpha} \rightarrow \delta = -\frac{\lambda}{\alpha} - \frac{2(1 - \alpha)}{\alpha}. \tag{B4}$$

(ii) $\Delta < 0$. The energy spectrum only has cross points with lower mobility edge line $E = \frac{2}{\alpha} - \frac{\lambda}{\alpha}$. When $|\Delta|$ is small, the approximate range of energy spectrum is $[-2 + \frac{\Delta}{1+\alpha} - \frac{\lambda}{\alpha}, 2 + \frac{\Delta}{1-\alpha} - \frac{\lambda}{\alpha}]$. So the transition point upon which the mobility edge line meets the energy spectrum is determined by

$$\frac{2}{\alpha} = -2 + \frac{\Delta}{1 + \alpha} \tag{B5}$$

and the transition point is

$$\Delta = \frac{2(1 + \alpha)^2}{\alpha} \rightarrow \delta = -\frac{\lambda}{\alpha} + \frac{2(1 + \alpha)^2}{\alpha}. \tag{B6}$$

When $|\Delta|$ is large, all the eigenstates become localized states. In this region, $[\frac{\Delta}{1+\alpha} - \frac{\lambda}{\alpha}, \frac{\Delta}{1-\alpha} - \frac{\lambda}{\alpha}]$ is a good approximation for the range of energy spectrum. And the transition point where all the states become localized is determined by

$$\frac{2}{\alpha} = \frac{\Delta}{1 - \alpha} \tag{B7}$$

and thus the transition point given as

$$\Delta = \frac{2(1 - \alpha)}{\alpha} \rightarrow \delta = -\frac{\lambda}{\alpha} + \frac{2(1 - \alpha)}{\alpha}. \tag{B8}$$

One can find that these transition points are symmetric about $\delta = -\frac{\lambda}{\alpha}$. As δ varies, we can obtain systems which are fully localized, partially localized, and fully extended. For

intervals of δ possessing true mobility edges, it is worth noting that when $\Delta < 0$, the low-energy eigenstates are localized and the high-energy eigenstates are extended, while contrarily the situation reverses when $\Delta > 0$.

---

[1] P. W. Anderson, Absence of diffusion in certain random lattices, Phys. Rev. **109**, 1492 (1958).

[2] E. Abrahams, P. W. Anderson, D. C. Licciardello, and T. V. Ramakrishnan, Scaling theory of localization: Absence of quantum diffusion in two dimensions, Phys. Rev. Lett. **42**, 673 (1979).

[3] N. Mott, The mobility edge since 1967, J. Phys. C: Solid State Phys. **20**, 3075 (1987).

[4] P. A. Lee and T. V. Ramakrishnan, Disordered electronic systems, Rev. Mod. Phys. **57**, 287 (1985).

[5] S. Aubry and G. André, Analyticity breaking and Anderson localization in incommensurate lattices, Ann. Isr. Phys. Soc. **3**, 133 (1980).

[6] D. J. Thouless, Localization by a potential with slowly varying period, Phys. Rev. Lett. **61**, 2141 (1988).

[7] M. Kohmoto, Metal-insulator transition and scaling for incommensurate systems, Phys. Rev. Lett. **51**, 1198 (1983).

[8] M. Kohmoto and D. Tobe, Localization problem in a quasiperiodic system with spin-orbit interaction, Phys. Rev. B **77**, 134204 (2008).

[9] X. Cai, L.-J. Lang, S. Chen, and Y. Wang, Topological superconductor to anderson localization transition in one-dimensional incommensurate lattices, Phys. Rev. Lett. **110**, 176403 (2013).

[10] G. Roati, C. D'Errico, L. Fallani, M. Fattori, C. Fort, M. Zaccanti, G. Modugno, M. Modugno, and M. Inguscio, Anderson localization of a non-interacting Bose-Einstein condensate, Nature (London) **453**, 895 (2008).

[11] Y. Lahini, R. Pugatch, F. Pozzi, M. Sorel, R. Morandotti, N. Davidson, and Y. Silberberg, Observation of a localization transition in quasiperiodic photonic lattices, Phys. Rev. Lett. **103**, 013901 (2009).

[12] S. Ganeshan, J. H. Pixley, and S. Das Sarma, Nearest neighbor tight binding models with an exact mobility edge in one dimension, Phys. Rev. Lett. **114**, 146601 (2015).

[13] H. P. Lüschen, S. Scherg, T. Kohlert, M. Schreiber, P. Bordia, X. Li, S. Das Sarma, and I. Bloch, Single-particle mobility edge in a one-dimensional quasiperiodic optical lattice, Phys. Rev. Lett. **120**, 160404 (2018).

[14] Y. Wang, X. Xia, L. Zhang, H. Yao, S. Chen, J. You, Q. Zhou, and X.-J. Liu, One-dimensional quasiperiodic mosaic lattice with exact mobility edges, Phys. Rev. Lett. **125**, 196604 (2020).

[15] J. Gao, I. M. Khaymovich, X.-W. Wang, Z.-S. Xu, A. Iovan, G. Krishna, A. V. Balatsky, V. Zwiller, and A. W. Elshaari, Experimental probe of multi-mobility edges in quasiperiodic mosaic lattices, arXiv:2306.10829.

[16] S. Das Sarma, S. He, and X. C. Xie, Mobility edge in a model one-dimensional potential, Phys. Rev. Lett. **61**, 2144 (1988).

[17] S. Das Sarma, S. He, and X. C. Xie, Localization, mobility edges, and metal-insulator transition in a class of one-dimensional slowly varying deterministic potentials, Phys. Rev. B **41**, 5544 (1990).

[18] J. Biddle and S. Das Sarma, Predicted mobility edges in one-dimensional incommensurate optical lattices: An exactly solvable model of Anderson localization, Phys. Rev. Lett. **104**, 070601 (2010).

[19] M. Gonçalves, B. Amorim, E. V. Castro, and P. Ribeiro, Hidden dualities in 1D quasiperiodic lattice models, SciPost Phys. **13**, 046 (2022).

[20] M. Gonçalves, B. Amorim, E. V. Castro, and P. Ribeiro, Renormalization group theory of one-dimensional quasiperiodic lattice models with commensurate approximants, Phys. Rev. B **108**, L100201 (2023).

[21] D. D. Vu and S. Das Sarma, Generic mobility edges in several classes of duality-breaking one-dimensional quasiperiodic potentials, Phys. Rev. B **107**, 224206 (2023).

[22] M. Gonçalves, B. Amorim, E. V. Castro, and P. Ribeiro, Critical phase dualities in 1D exactly-solvable quasiperiodic models, arXiv:2208.07886.

[23] M. Gonçalves, J. H. Pixley, B. Amorim, E. V. Castro, and P. Ribeiro, Short-range interactions are irrelevant at the quasiperiodic-driven Luttinger Liquid to Anderson Glass transition, arXiv:2304.09197.

[24] Y. Hashimoto, K. Niizeki, and Y. Okabe, A finite-size scaling analysis of the localization properties of one-dimensional quasiperiodic systems, J. Phys. A: Math. Gen. **25**, 5211 (1992).

[25] D. J. Boers, B. Goedeke, D. Hinrichs, and M. Holthaus, Mobility edges in bichromatic optical lattices, Phys. Rev. A **75**, 063404 (2007).

[26] J. Biddle, B. Wang, D. J. Priour, and S. Das Sarma, Localization in one-dimensional incommensurate lattices beyond the Aubry-André model, Phys. Rev. A **80**, 021603(R) (2009).

[27] S. Lellouch and L. Sanchez-Palencia, Localization transition in weakly interacting Bose superfluids in one-dimensional quasiperdiodic lattices, Phys. Rev. A **90**, 061602(R) (2014).

[28] J. Biddle, D. J. Priour, B. Wang, and S. Das Sarma, Localization in one-dimensional lattices with non-nearest-neighbor hopping: Generalized Anderson and Aubry-André models, Phys. Rev. B **83**, 075105 (2011).

[29] X. Li, J. H. Pixley, D.-L. Deng, S. Ganeshan, and S. Das Sarma, Quantum nonergodicity and fermion localization in a system with a single-particle mobility edge, Phys. Rev. B **93**, 184204 (2016).

[30] X. Li, X. Li, and S. Das Sarma, Mobility edges in one-dimensional bichromatic incommensurate potentials, Phys. Rev. B **96**, 085119 (2017).

[31] X. Deng, S. Ray, S. Sinha, G. V. Shlyapnikov, and L. Santos, One-dimensional quasicrystals with power-law hopping, Phys. Rev. Lett. **123**, 025301 (2019).

[32] M. Saha, S. K. Maiti, and A. Purkayastha, Anomalous transport through algebraically localized states in one dimension, Phys. Rev. B **100**, 174201 (2019).

[33] S. Roy, T. Mishra, B. Tanatar, and S. Basu, Reentrant localization transition in a quasiperiodic chain, Phys. Rev. Lett. **126**, 106803 (2021).

[34] D. Dwiputra and F. P. Zen, Single-particle mobility edge without disorder, Phys. Rev. B **105**, L081110 (2022).

[35] H. Yao, T. Giamarchi, and L. Sanchez-Palencia, Lieb-liniger bosons in a shallow quasiperiodic potential: Bose glass phase and fractal Mott lobes, Phys. Rev. Lett. **125**, 060401 (2020).

[36] T. Liu, X. Xia, S. Longhi, and L. Sanchez-Palencia, Anomalous mobility edges in one-dimensional quasiperiodic models, SciPost Phys. **12**, 027 (2022).

[37] A. Duthie, S. Roy, and D. E. Logan, Self-consistent theory of mobility edges in quasiperiodic chains, Phys. Rev. B **103**, L060201 (2021).

[38] Y. Wang, X. Xia, Y. Wang, Z. Zheng, and X.-J. Liu, Duality between two generalized Aubry-André models with exact mobility edges, Phys. Rev. B **103**, 174205 (2021).

[39] Y.-C. Zhang and Y.-Y. Zhang, Lyapunov exponent, mobility edges, and critical region in the generalized Aubry-André model with an unbounded quasiperiodic potential, Phys. Rev. B **105**, 174206 (2022).

[40] Z.-H. Xu, X. Xia, and S. Chen, Exact mobility edges and topological phase transition in two-dimensional non-Hermitian quasicrystals, Sci. China: Phys., Mech. Astron. **65**, 227211 (2022).

[41] C. Chiaracane, M. T. Mitchison, A. Purkayastha, G. Haack, and J. Goold, Quasiperiodic quantum heat engines with a mobility edge, Phys. Rev. Res. **2**, 013093 (2020).

[42] V. Balachandran, S. R. Clark, J. Goold, and D. Poletti, Energy current rectification and mobility edges, Phys. Rev. Lett. **123**, 020603 (2019).

[43] M. Saha and S. K. Maiti, Particle current rectification in a quasi-periodic double-stranded ladder, J. Phys. D: Appl. Phys. **52**, 465304 (2019).

[44] C. Yuce and H. Ramezani, Coexistence of extended and localized states in the one-dimensional non-Hermitian Anderson model, Phys. Rev. B **106**, 024202 (2022).

[45] T. Liu and X. Xia, Real-complex transition driven by quasiperiodicity: A class of non-$\mathcal{PT}$ symmetric models, Phys. Rev. B **105**, 054201 (2022).

[46] W. Han and L. Zhou, Dimerization-induced mobility edges and multiple reentrant localization transitions in non-Hermitian quasicrystals, Phys. Rev. B **105**, 054204 (2022).

[47] W. Chen, S. Cheng, J. Lin, R. Asgari, and G. Xianlong, Breakdown of the correspondence between the real-complex and delocalization-localization transitions in non-Hermitian quasicrystals, Phys. Rev. B **106**, 144208 (2022).

[48] Y. Liu, X.-P. Jiang, J. Cao, and S. Chen, Non-Hermitian mobility edges in one-dimensional quasicrystals with parity-time symmetry, Phys. Rev. B **101**, 174205 (2020).

[49] X. Cai, Localization and topological phase transitions in non-Hermitian Aubry-André-Harper models with *p*-wave pairing, Phys. Rev. B **103**, 214202 (2021).

[50] S. Longhi, Metal-insulator phase transition in a non-Hermitian Aubry-André-Harper model, Phys. Rev. B **100**, 125157 (2019).

[51] Q. Tang and Y. He, Mobility edges in one-dimensional models with quasi-periodic disorder, J. Phys.: Condens. Matter **33**, 185505 (2021).

[52] Y. Liu, Y. Wang, X.-J. Liu, Q. Zhou, and S. Chen, Exact mobility edges, $\mathcal{PT}$-symmetry breaking, and skin effect in one-dimensional non-Hermitian quasicrystals, Phys. Rev. B **103**, 014203 (2021).

[53] A. Avila, Global theory of one-frequency Schrödinger operators, Acta Math. **215**, 1 (2015).

[54] Y. Liu, Y. Wang, Z. Zheng, and S. Chen, Exact non-Hermitian mobility edges in one-dimensional quasicrystal lattice with exponentially decaying hopping and its dual lattice, Phys. Rev. B **103**, 134208 (2021).

[55] Y. Liu, Q. Zhou, and S. Chen, Localization transition, spectrum structure, and winding numbers for one-dimensional non-Hermitian quasicrystals, Phys. Rev. B **104**, 024201 (2021).

[56] D. J. Thouless, Electrons in disordered systems and the theory of localization, Phys. Rep. **13**, 93 (1974).

[57] D. J. Thouless, A relation between the density of states and range of localization for one dimensional random systems, J. Phys. C: Solid State Phys. **5**, 77 (1972).

[58] X. Li and S. Das Sarma, Mobility edge and intermediate phase in one-dimensional incommensurate lattice potentials, Phys. Rev. B **101**, 064203 (2020).

[59] B. Simon and T. Spencer, Trace class perturbations and the absence of absolutely continuous spectra, Commun. Math. Phys. **125**, 113 (1989).

[60] F. A. An, E. J. Meier, and B. Gadway, Engineering a flux-dependent mobility edge in disordered zigzag chains, Phys. Rev. X **8**, 031045 (2018).

[61] T. Kohlert, S. Scherg, X. Li, H. P. Lüschen, S. Das Sarma, I. Bloch, and M. Aidelsburger, Observation of many-body localization in a one-dimensional system with a single-particle mobility edge, Phys. Rev. Lett. **122**, 170403 (2019).

[62] F. A. An, K. Padavić, E. J. Meier, S. Hegde, S. Ganeshan, J. H. Pixley, S. Vishveshwara, and B. Gadway, Interactions and mobility edges: Observing the generalized Aubry-André model, Phys. Rev. Lett. **126**, 040603 (2021).

[63] Y. Wang, J.-H. Zhang, Y. Li, J. Wu, W. Liu, F. Mei, Y. Hu, L. Xiao, J. Ma, C. Chin, and S. Jia, Observation of interaction-induced mobility edge in an atomic Aubry-André wire, Phys. Rev. Lett. **129**, 103401 (2022).

[64] B. Gadway, Atom-optics approach to studying transport phenomena, Phys. Rev. A **92**, 043606 (2015).

[65] M. Verbin, O. Zilberberg, Y. Lahini, Y. E. Kraus, and Y. Silberberg, Topological pumping over a photonic Fibonacci quasicrystal, Phys. Rev. B **91**, 064201 (2015).